Evaluation of ultrasound scattering models adapted for two types of scatterers to extract scatterer parameters from cell-pellet biophantoms

Pauline Muleki Seya, Aiguo Han, William O'Brien

Evaluation of ultrasound scattering models adapted for two types of scatterers to extract scatterer parameters from cell-pellet biophantoms

Pauline Muleki-Seya
CNRS, Université de Lyon, INSA CREATIS
69100 Villeurbanne, France
pauline.muleki-seya@creatis.insa-lyon.fr

Aiguo Han
ECE Department, University of Illinois Bioacoustics Research Laboratory
61801 Urbana, USA
han51@illinois.edu

William D. O'Brien, Jr.
ECE Department, University of Illinois Bioacoustics Research Laboratory
61801 Urbana, USA
wdo@uiuc.edu

***Abstract*—Ultrasound backscatter coefficient allows the evaluation of tissue microstructure parameters. Scatterer parameters are then extracted using ultrasound scattering models. It is generally difficult to correlate the scatterer parameters to tissue structures from histology, possibly because of inappropriate scattering models or the presence of multiple scatterers. In previous work, we used an adaptation of the scattering Structure Factor Model (SFM) to take into account two types of scatterers (nuclei and cells) using a combination of SFM from nuclei and SFM from cells. Our results suggested the contribution of both nuclei and cells in the scattering. The objective of this study is to explore the possibility to extract coherent scatterer parameters with scattering models taking into account two types of scatterers: the adapted SFM for two scatterers' types and the concentric sphere model.**

***Index Terms*—Quantitative ultrasound techniques, Ultrasound scattering, cell pellet biophantoms, Scatterer parameters**

I. Introduction

The backscatter coefficient (BSC) contains inherent properties of tissue microstructure. This kind of information from tissue may be valuable when tissue microstructure is affected: in presence of fat droplets in the liver for non-alcoholic fatty liver disease patients [1], cell-death changes (condensation and fragmentation of nuclei and cells via apoptosis) during anti-cancer therapy [2], tissue/tumor alteration during HIFU heating treatment [3], comparison between cancerous and healthy tissues [4].

Using an inverse problem approach, it is possible to extract scatterer parameters from BSC as the scatterer's radius and the acoustic concentration when the Gaussian model (GM) or the fluid sphere model [5] is used. These models deal with identical randomly and independently distributed scatterers, making them valid only for diluted medium. It is generally difficult to correlate the scatterer parameters to tissue structures from histology [6]. The structure factor model (SFM) [7], [8], combining the contributions of the incoherent and coherent BSC, is adapted for concentrated medium. With this model, it is possible to extract the scatterer radius and volume fraction and its relative impedance contrast. The use of SFM yields scatterer parameters close to cellular structures: nuclei for canine liver (with a relative error on radius and volume fraction $<7\%$) and whole cells for HT29 tumors (with a relative error on radius and volume fraction $<15\%$) [9]. In another study [10], the mean relative errors on scatterer radius and volume fraction were $<14\%$ (17%, respectively) for LMTK (MAT, respectively) cell-pellet (CP) biophantoms and mean relative errors $<5\%$ on radius for 4T1, JC, LMTK and MAT *ex vivo* tumors. However, the mean relative errors were not satisfying for 4T1 and JC CP, probably because of scattering not only from either cells or nuclei but also from both cells and nuclei. In that case, an appropriate model to extract scatterer parameters should take into account the scattering from both cells and nuclei.

To evaluate scattering from both cells and nuclei, the BSC was considered as a linear contribution of the BSC from nuclei and cells with a nucleus-to-cell scattering ratio term [10]. The BSCs from nuclei and cells were estimated using SFM using radii and volume fractions for nuclei and cells from histological images. This model considered 7 parameters (radius, volume fraction, relative impedance contrast from "nuclei" and "cells" scatterers, and the nucleus-to-cell scattering ratio). The concentric spheres model (CSM) [11] considered the incoherent scattering from an ensemble of concentric fluid spheres. This model considered 9 parameters (inner and outer radius, density and sound speed of the background, inner and outer spheres, and scatterer number density). CSM provided consistent results when compared with experimental acquisitions of sparse CHO biophantoms [12], [13]. This model provided a better representation of 4T1 and MAT cell-pellet biophantoms and *ex vivo* tumors rather than a single fluid sphere model [14].

The objective of this study is to determine if more pertinent scatterer parameters could be estimated from models by taking into account two types of scatterers (nuclei and cells) rather than monodisperse scatterers. For that, scatterer parameters

NIH Support: R01CA226528.

from 4 cell lines of CP were estimated using the monodisperse SFM, SFM adapted for two scatterers and the CSM.

II. Material and Methods

A. Ultrasound acquisitions

The CP biophantoms were composed of a large number of densely packed cells without any supportive background materials. Four tumor cell lines were used to create the CP biophantoms: 13762 MAT B III (MAT) mammary adenocarcinoma (ATCC CRL-1666), 4T1 mammary carcinoma (ATCC CRL-2539), JC mammary adenocarcinoma (ATCC CRL-2116) and LMTK soft-tissue sarcoma (ATCC CCL-1.3), denoted MAT, 4T1, JC and LMTK, respectively. The experimental procedure to fabricate CP biophantoms has been described in [14]. 3 MAT, 16 4T1, 10 JC, and 15 LMTK independent CP replicates were ultrasonically scanned and analyzed.

Ultrasound acquisitions were realized with a single-element, weakly focused 40-MHz transducer (High-Frequency Transducer Resource Center, USC, Los Angeles, CA, -10 dB bandwidth of 25–55 MHz). The scanning procedure [14] was composed of the acquisition of the radio-frequency (RF) signals and attenuation measurements (insertion-loss broadband technique [15]). For each sample, 11 independent scans were recorded. A mean BSC was estimated for each of the 11 scans by averaging the BSCs from all the ROIs within that scan. Then, for each CP, 11 mean BSCs were extracted and used to estimate the scatterer parameters. Immediately after scanning, the sample was prepared for histology processing. Cell and nucleus radii and volume fractions were estimated from histological images of these CP [10].

B. Ultrasound scattering models

This paper compared QUS estimates from three models: SFM, SFM adapted for 2 scatterers (denoted SFM2) and CSM. SFM considers an ensemble of identical fluid spheres. This model is adapted for concentrated media by taking into account the Structure Factor term S related to scatterer spatial positions. SFM is based on the assumption that, at high scatterer volume fractions, interference effects are mainly caused by correlations between the spatial positions of individual scatterers. By considering an ensemble of identical spheres of radius a, the theoretical BSC for the SFM formulation is given by [7], [8]:

$$BSC_{SFM}(k) = n\frac{k^4 V_s^2 \gamma_Z^2}{4\pi^2}[\frac{3}{(2ka)^3}j_1(2ka)]^2 S(k); \quad (1)$$

where k is the wavenumber, V_s is the sphere volume and $n = \phi/V_s$ is the number density with ϕ the scatterer volume fraction, γ_Z is the relative impedance contrast between the scatterer and the surrounding medium and j_1 is the spherical Bessel function of the first kind of order 1. S is the structure factor, which is analytically obtained as described in [8], [16]. The unknown parameters are the scatterer radius a, the volume fraction ϕ, and the relative impedance contrast γ_Z.

For the optical H&E-stained histology images, the nuclei colors in the RGB images may be quite variable, suggesting that the nuclei acoustic impedance may be quite variable from one nucleus to another. Therefore, it is possible that for some cells, the main ultrasonic scattering sites are the nuclei and for others, the cells themselves. In these conditions, the BSC from cells and nuclei BSC_{NC} using SFM2 is defined as [10]:

$$BSC_{NC}(k) = wBSC_N(k) + (1-w)BSC_C(k) \quad (2)$$

where BSC_N and BSC_C are the BSCs from nuclei and cells only estimated with SFM (eq 1) and w is the nucleus-to-cell scattering ratio: $w = 0$ corresponds to scattering from cells only and $w = 1$ corresponds to scattering from nuclei only. The unknown parameters are the scatterer radii a_N and a_C, the volume fractions ϕ_N and ϕ_C, the relative impedance contrasts γ_{Z_N} and γ_{Z_C} and the nucleus-to-cell scattering ratio w. Because of the presence of the term w, the relative impedance contrasts estimated do not correspond to the relative impedance contrast estimated with SFM.

The CSM considers an ensemble of randomly positioned concentric-sphere scatterers (inner sphere denoted 2, outer sphere denoted 1 and background denoted 0). By assuming the coherent field is not taken into account and waves do not interfere, the BSC is written as [12]:

$$BSC_{CSM}(f) = nr^2\frac{|p_{scatt}(\theta=\pi)|^2}{P_0^2} \quad (3)$$

where f is the frequency, r is the observation point, $p_{scatt}(\theta = \pi)$ is the backscattered acoustic pressure and P_0 is the amplitude of the incident pressure. At an observation point r, the acoustic pressure scattered from the two concentric spheres is given in [11]. The unknown parameters are the inner and outer scatterer radii a_2 and a_1, the densities (ρ_0, ρ_1, ρ_2), the sound speeds (c_0, c_1, c_2), and the number density n. The outer and inner volume fractions were evaluated as:

$$\phi_1 = 4\pi a_1^3 n \quad (4)$$

$$\phi_2 = 4\pi a_2^3 n \quad (5)$$

Estimated values of the scatterer parameters were determined by fitting the measured BSC_{meas} to the theoretical BSCs, BSC_{theo}, by minimizing the cost function:

$$F = \frac{\sum_j \|BSC_{meas}(k_j) - BSC_{theo}(k_j)\|^2}{\sum_j BSC_{meas}(k_j)^2} \quad (6)$$

where BSC_{theo} is given by eq. 1, 2 or 3. The cost functions were minimized over 25–55 MHz. The fitting procedure was performed using the minimization routine *fminsearch* without constraint and *fmincon* with constraints in MATLAB (The MathWorks, Inc., Natick, MA). The constraints used for SFM were $3 < a < 10$ μm, $0.05 < \phi < 0.8$, and $0 < \gamma_Z < 0.2$. The constraints used for SFM2 were

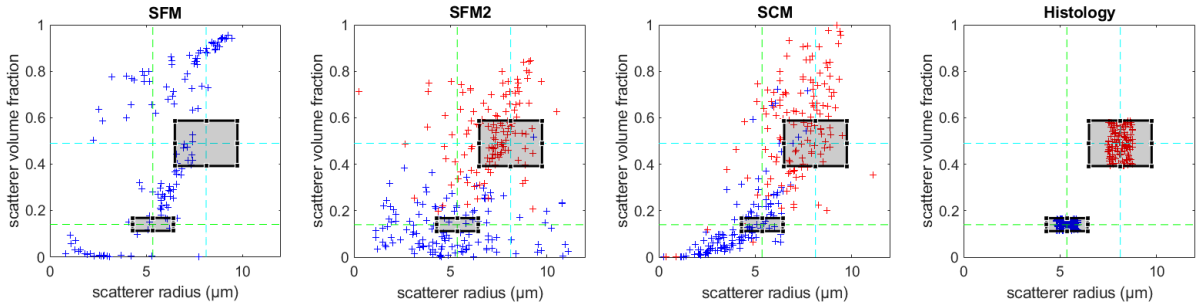

Fig. 1. Scatterer radius vs volume fraction for 4T1 CP obtained with SFM, SFM2 and CSM without constraints (fminsearch) and extracted from histology. Blue cross: scatterers corresponding to nuclei, red cross: scatterers corresponding to cells. The black rectangles areas correspond to the areas of the correct nucleus and cell estimations.

$3 < a_N < 6.5$ μm, $5.5 < a_C < 10$ μm, $0.05 < \phi_N < 0.3$, $0.4 < \phi_C < 0.8$, $0 < \gamma_{ZN} < 0.2$, $0 < \gamma_{ZC} < 0.2$ and $0 < w < 1$. The constraints used for CSM were $3 < a_2 < 6.5$ μm, $5.5 < a_1 < 10$ μm, $0.9 < \rho_{0,1,2} < 1.2$, $1450 < c_{0,1,2} < 1630$, and $40 < n < 2700$. The best cost function was evaluated by testing 20 initial conditions .

III. Results and Discussion

A (a,ϕ) distribution example for 4T1 CP is presented in Figure 1. With SFM, the (a,ϕ) distribution is variable and does not seem to be centered around nucleus or cell values. The models adapted for 2 scatterers allow two (a,ϕ) distributions with mean values more or less around the mean nucleus and cell radii and volume fractions estimated from histology.

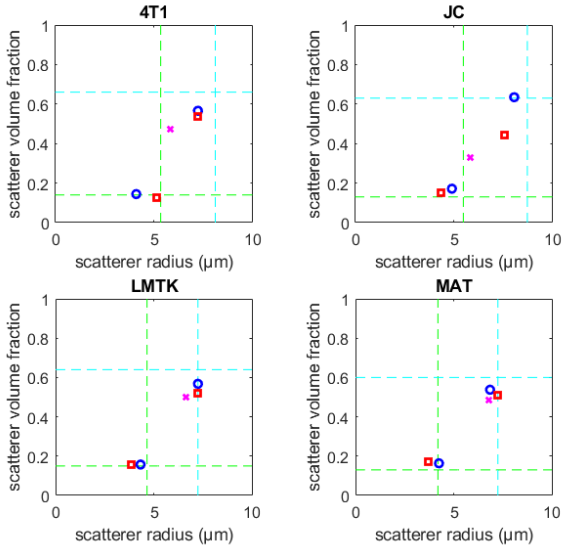

Fig. 2. Mean scatterer parameter values obtained with SFM (magenta cross), SFM2 (red squares) and CSM (blue circles) without constraints (fminsearch) for 4T1, JC, LMTK and MAT CP. The green and cyan lines correspond to the mean nucleus and cell radii and volume fractions from histology.

Mean scatterer parameter values obtained with SFM, SFM2 and CSM for the 4 cell lines are presented in Figure 2 along with the mean nucleus and cell radii and volume fractions from histology using the optimization strategy without constraints. In all cases, one of the other model adapted for two scatterers provided mean parameters closer to histology values. For 4T1 for example, SFM provides scatterer values with a relative error of 9.5% (4.0% for SFM2 and 23.1% for CSM, respectively) on nucleus radii, 239.3% (9.8% for SFM2 and 3.0% for CSM, respectively) on nucleus volume fractions, 27.9% (11.2% for SFM2 and 10.9% for CSM, respectively) on cell radii and 28.0% (18.8% for SFM2 and 14.3% for CSM, respectively) on cell volume fractions. Using constraints makes it possible to reduce these average relative errors but to the detriment of one or more parameters generally. For MAT, SFM2 without constraints provides scatterer values with a relative error of 11.9% (1,2% with constraints, respectively) on nucleus radii, 31.9% (25.8% with constraints, respectively) on nucleus volume fractions, 0.4% (5.5% with constraints, respectively) on cell radii and 20.3% (16.0% with constraints, respectively) on cell volume fractions.

The variability of scatterer parameter distribution was estimated using the coefficient of variation (ratio of the standard deviation to the mean). Scattering models adapted for two scatterers (SFM2 and CSM) do not reduce the coefficient of variation of the estimates. For 4T1, SFM provided coefficient of variation of 36.5% (48.7% and 23.0% for SFM2, 41.1% and 23.0% for CSM, respectively) for the radius and 69.3% (77.6% and 28.0% for SFM2, 108.7% and 38.0% for CSM, respectively) for the volume fraction. Using constraints tend to reduce the coefficient of variation, but sometimes to the detriment of one or several parameters. For MAT, SFM2 without constraints provided coefficient of variation of 11.9% and 0.4% (1.3% and 3.2% with constraints, respectively) for the radius and 31.9% and 20.3% (42.6% and 9.6% with constraints, respectively) for the volume fraction.

”Correct” nucleus and cell estimates were defined as scatterer radius and volume fraction estimated both (for

	Without constraints						With constraints					
	SFM		SFM2		CSM		SFM		SFM2		CSM	
	Nuclei	Cells	Nuclei	Cells	Nuclei	Cells	Nuclei	Cells	Nuclei	Cells	Nuclei	Cells
4T1	3.8	8.3	2.3	38.6	9.9	22.0	3.0	6.1	6.8	27.3	6.6	10.6
JC	0.9	0.0	1.8	36.4	10.0	23.6	0.9	0.0	7.3	40.0	8.2	4.4
LMTK	1.2	2.4	4.9	35.8	6.7	33.3	2.4	6.7	10.3	40.6	17.6	11.5
MAT	0.0	9.1	0.0	48.5	9.1	42.4	0.0	45.5	9.1	72.7	15.2	12.1

TABLE I

PERCENTAGE OF "CORRECT" NUCLEUS AND CELL ESTIMATES USING SFM, SFM2 AND CSM (WITH AND WITHOUT CONSTRAINTS) FOR 4T1, JC, LMTK AND MAT.

cells or nuclei) with less than 0.2 times the mean radius or volume fraction value (black rectangles areas in Figure 1). The percentage of "correct" nucleus and cell estimates with SFM, SFM2 and CSM with and without constraints in the optimization approach are summarized in Table I. SFM2 and CSM allow estimating a higher percentage of correct cell parameters. For example, for LMTK CP without constraints, 2.4% of correct cell parameters were estimated with SFM, 35.8% with SFM2 and 33.3% with CSM. Percentages of correct cell parameters are lower with CSM than with SFM2 but percentages of correct nuclei are higher. When using constraints (Table I), the percentage of correct estimates with SFM is not better except for MAT cells which increase from 9.1% to 45.5%. The percentage of correct nucleus parameters estimated with SFM2 increase and the percentage of correct cell parameters increase also for JC, LMTK and MAT but decrease for 4T1. Using constraints, the percentage of correct cell estimates is lower with CSM. It may be because of the choice of inappropriate sound speed and density constraints. With CSM, estimates with unrealistic values (i.e. $\phi < 1$) were observed. These estimates contribute to reduce the percentage of correct estimates. A strategy to take care of them has to be defined.

IV. CONCLUSION

In this study, we tested the ability of models adapted for two scatterers to estimate pertinent scatterer parameters on CP by comparing scatterer parameters extracted with SFM, SFM2 and CSM. The models adapted for two scatterers provided closer mean parameters when compared to the histological value and increases the percentage of correct nucleus and mainly cell estimates. However, they do not reduce the coefficients of variation of the radius and volume fraction estimates.

ACKNOWLEDGMENT

This research was supported by the NIH grant (R01CA226528). We thank Jamie Kelly and Jake Berndt for their help in ultrasound acquisitions.

REFERENCES

[1] S. C. Lin, E. Heba, T. Wolfson, B. Ang, A. Gamst, A. Han, J. W. Erdman, W. D. O'Brien, M. P. Andre, C. B. Sirlin, and R. Loomba, "Noninvasive Diagnosis of Nonalcoholic Fatty Liver Disease and Quantification of Liver Fat Using a New Quantitative Ultrasound Technique," *Clinical Gastroenterology and Hepatology*, vol. 13, no. 7, pp. 1337–1345.e6, 2015.

[2] M. C. Kolios, G. J. Czarnota, M. Lee, J. W. Hunt, and M. D. Sherar, "Ultrasonic spectral parameter characterization of apoptosis," *Ultrasound in Medicine & Biology*, vol. 28, no. 5, pp. 589–597, 2002.

[3] J. P. Kemmerer, G. Ghoshal, C. Karunakaran, and M. L. Oelze, "Assessment of high-intensity focused ultrasound treatment of rodent mammary tumors using ultrasound backscatter coefficients," *The Journal of the Acoustical Society of America*, vol. 134, no. 2, pp. 1559–1568, 2013.

[4] J. Mamou, A. Coron, M. L. Oelze, E. Saegusa-Beecroft, M. Hata, P. Lee, J. Machi, E. Yanagihara, P. Laugier, and E. J. Feleppa, "Three-Dimensional High-Frequency Backscatter and Envelope Quantification of Cancerous Human Lymph Nodes," *Ultrasound in Medicine & Biology*, vol. 37, no. 3, pp. 345–357, 2011.

[5] M. F. Insana, D. G. Brown, and K. K. Shung, "Acoustic scattering theory applied to soft biological tissues," in *Ultrasonic scattering in biological tissues*, pp. 75–124, CRC Press Boca Raton, FL, 1993.

[6] M. L. Oelze and W. D. O'Brien, "Application of Three Scattering Models to Characterization of Solid Tumors in Mice," *Ultrasonic Imaging*, vol. 28, no. 2, pp. 83–96, 2006.

[7] V. Twersky, "Low-frequency scattering by correlated distributions of randomly oriented particles," *The Journal of the Acoustical Society of America*, vol. 81, no. 5, pp. 1609–1618, 1987.

[8] E. Franceschini and R. Guillermin, "Experimental assessment of four ultrasound scattering models for characterizing concentrated tissue-mimicking phantoms," *The Journal of the Acoustical Society of America*, vol. 132, no. 6, pp. 3735–3747, 2012.

[9] P. Muleki-Seya, R. Guillermin, J. Guglielmi, J. Chen, T. Pourcher, E. Konofagou, and E. Franceschini, "High-Frequency Quantitative Ultrasound Spectroscopy of Excised Canine Livers and Mouse Tumors Using the Structure Factor Model," *IEEE Transactions on Ultrasonics, Ferroelectrics, and Frequency Control*, vol. 63, no. 9, pp. 1335–1350, 2016.

[10] P. Muleki-Seya and W. D. O'Brien, "Ultrasound Scattering From Cell-Pellet Biophantoms and Ex Vivo Tumors Provides Insight Into the Cellular Structure Involved in Scattering," *IEEE Transactions on Ultrasonics, Ferroelectrics, and Frequency Control*, vol. 69, no. 2, pp. 637–649, 2022.

[11] J. McNew, R. Lavarello, and W. D. O'Brien, "Sound scattering from two concentric fluid spheres," *The Journal of the Acoustical Society of America*, vol. 125, no. 1, pp. 1–4, 2009.

[12] M. Teisseire, A. Han, R. Abuhabsah, J. P. Blue, S. Sarwate, and W. D. O'Brien, "Ultrasonic backscatter coefficient quantitative estimates from Chinese hamster ovary cell pellet biophantoms," *The Journal of the Acoustical Society of America*, vol. 128, no. 5, pp. 3175–3180, 2010.

[13] A. Han, R. Abuhabsah, J. P. Blue, S. Sarwate, and W. D. O'Brien, "Ultrasonic backscatter coefficient quantitative estimates from high-concentration Chinese hamster ovary cell pellet biophantoms," *The Journal of the Acoustical Society of America*, vol. 130, no. 6, pp. 4139–4147, 2011.

[14] A. Han, R. Abuhabsah, R. J. Miller, S. Sarwate, and W. D. O'Brien, "The measurement of ultrasound backscattering from cell pellet biophantoms and tumors ex vivo," *The Journal of the Acoustical Society of America*, vol. 134, no. 1, pp. 686–693, 2013.

[15] K. A. Wear, T. A. Stiles, G. R. Frank, E. L. Madsen, F. Cheng, E. J. Feleppa, C. S. Hall, B. S. Kim, P. Lee, W. D. O. Brien, M. L. Oelze, B. I. Raju, K. K. Shung, T. A. Wilson, and J. R. Yuan, "Interlaboratory Comparison of Ultrasonic Backscatter Coefficient Measurements From 2 to 9 MHz," *Journal of Ultrasound in Medicine*, vol. 24, no. 9, pp. 1235–1250, 2005.

[16] M. S. Wertheim, "Exact Solution of the Percus-Yevick Integral Equation for Hard Spheres," *Physical Review Letters*, vol. 10, no. 8, pp. 321–323, 1963.